THE JOURNAL OF BIOLOGICAL CHEMISTRY
Vol. 280, No. 12, Issue of March 25, pp. 11608–11614, 2005

*Printed in U.S.A.*

# A Novel Isoform of the Secretory Pathway $Ca^{2+}$,$Mn^{2+}$-ATPase, hSPCA2, Has Unusual Properties and Is Expressed in the Brain*

Received for publication, November 19, 2004, and in revised form, January 21, 2005
Published, JBC Papers in Press, January 27, 2005, DOI 10.1074/jbc.M413116200

**Minghui Xiang, Deepti Mohamalawari, and Rajini Rao‡**

*From the Department of Physiology, The Johns Hopkins University School of Medicine, Baltimore, Maryland 21205*

**Unlike lower eukaryotes, mammalian genomes have a second gene, *ATP2C2*, encoding a putative member of the family of secretory pathway $Ca^{2+}$,$Mn^{2+}$-ATPases, SPCA2. Human SPCA2 shares 64% amino acid identity with the protein defective in Hailey Hailey disease, hSPCA1. We show that human SPCA2 (hSPCA2) has a more limited tissue distribution than hSPCA1, with prominent protein expression in brain and testis. In primary neuronal cells, endogenous SPCA2 has a highly punctate distribution that overlaps with vesicles derived from the *trans*-Golgi network and is thus different from the compact perinuclear distribution of hSPCA1 seen in keratinocytes and nonpolarized cells. Heterologous expression in a yeast strain lacking endogenous $Ca^{2+}$ pumps reveals further functional differences from hSPCA1. Although the $Mn^{2+}$-specific phenotype of hSPCA2 is similar to that of hSPCA1, $Ca^{2+}$ ions are transported with much poorer affinity, resulting in only weak complementation of $Ca^{2+}$-specific yeast phenotypes. These observations suggest that SPCA2 may have a more specialized role in mammalian cells, possibly in cellular detoxification of $Mn^{2+}$ ions, similar to that in yeast. We point to the close links between manganese neurotoxicity and Parkinsonism that would predict an important physiological role for SPCA2 in the brain.**

The secretory pathway $Ca^{2+}$-ATPases (SPCA(s))[1] are a recently recognized family of ion pumps that supply the lumen of the Golgi with divalent cations requisite for protein sorting, processing, and quality control (reviewed in Refs. 1 and 2). The founding member of this family, Pmr1 (for plasma membrane ATPase-related) was first described in the yeast *Saccharomyces cerevisiae* (3, 4), and shortly thereafter, a closely related gene (50% protein identity) was cloned from rat (5). Pmr1 was shown to be biochemically distinct from the well known $Ca^{2+}$-ATPases that reside in the sarcoendoplasmic reticulum (SERCA) and plasma membrane (PMCA) of higher eukaryotes (6). Of particular interest, Pmr1 has an unusual selectivity toward $Mn^{2+}$ ions and plays a prominent role in cellular detoxification of this trace element as well as in $Mn^{2+}$ delivery to the Golgi lumen, where it is an essential cofactor for endoglycosidases (7–10). Also noteworthy is the strikingly high affinity of Pmr1 for $Ca^{2+}$ and $Mn^{2+}$ ions, indicated by $K_m$ values of less than 0.1 $\mu$M for ion transport and ion-dependent ATP hydrolysis activity (9, 11).

Single orthologues of *PMR1* are found in the genomes of nematodes and *Drosophila*, whereas there are two paralogous genes in mammals, including humans. Heterologous expression studies of *C. elegans* PMR1 and human SPCA1 in COS1 cells and in yeast have confirmed $Mn^{2+}$ transport ability and a similar high affinity for $Ca^{2+}$ in the range of 0.25 $\mu$M, suggesting that these are shared features of the SPCA family (12–14). Haploinsufficiency of hSPCA1, caused by mutations in one allele of the *ATP2C1* gene, leads to Hailey Hailey disease, a debilitating blistering disorder of the skin characterized by disruption of desmosomal contacts in keratinocytes (15, 16). Other physiological roles of the SPCA include secretion of calcium into milk (17) and, potentially, into bone and teeth. Based on the known properties of these transporters, the SPCA family is likely to be important for uptake, detoxification, and homeostasis of calcium and manganese in the intestine, liver, and brain, respectively. However, molecular aspects of mammalian SPCA function remain to be determined, and experimental evidence for their physiological role is scarce.

The widespread expression pattern of SPCA1 and the absence of homozygous mutations in the *ATP2C1* gene are both consistent with an essential housekeeping role for this isoform (15). In contrast, a cDNA clone from human brain, KIAA0703, corresponding to a second SPCA isoform, was reported to have a more limited tissue distribution (18). Initial attempts to evaluate the function of this clone failed[2] and appeared to be due to an incorrect N-terminal sequence, presumably the result of a cloning artifact. We now report that the corrected clone encodes a functional SPCA pump that clearly differs from hSPCA1 in its ability to complement the phenotypes of a *pmr1* null strain of yeast. Biochemical characterization of hSPCA2 in yeast and subcellular localization in primary hippocampal cells reveal novel properties that may contribute to a distinct physiological role.

## MATERIALS AND METHODS

*Plasmids, Yeast Strains, and Growth Medium*—Plasmids pKT17yE, expressing the $His_9$-tagged long N-terminal splice variant of hSPCA1, and YEpHisPMR1, expressing $His_9$-tagged *S. cerevisiae* PMR1 have been described before (11, 19). cDNA clone KIAA0703 (gift of the Kazusa Research Institute, Japan) was amplified by polymerase chain reaction to include an N-terminal MluI site immediately prior to codon 1 (ATG) and a NotI site following the termination codon and subsequently cloned into the equivalent sites of plasmid pSM1052 (gift from Susan Michaelis, The Johns Hopkins University). This placed the open reading frame behind a $His_9$ epitope tag and under control of the

* This work was supported by National Institutes of Health Grant GM62142 and a grant-in-aid from the American Heart Association Mid-Atlantic affiliate (to R. R.). The costs of publication of this article were defrayed in part by the payment of page charges. This article must therefore be hereby marked "*advertisement*" in accordance with 18 U.S.C. Section 1734 solely to indicate this fact.

‡ To whom correspondence should be addressed: Dept. of Physiology, The Johns Hopkins University School of Medicine, 725 N. Wolfe St., Baltimore, MD 21205. Tel.: 410-955-4732; Fax: 410-955-0461; E-mail: rrao@jhmi.edu.

[1] The abbreviations used are: SPCA, secretory pathway $Ca^{2+}$-ATPase; hSPCA, human SPCA; BAPTA, 1,2-bis(2-aminophenoxy)ethane-*N*,*N*,*N*′,*N*′-tetraacetate; MES, 2-(*N*-morpholino)ethanesulfonic acid; PMCA, plasma membrane $Ca^{2+}$-ATPase; SERCA, sarcoendoplasmic reticulum $Ca^{2+}$-ATPase; TGN, *trans*-Golgi network.

[2] Y. Wei, D. Mandal, and R. Rao, unpublished results.

constitutive *PGK1* promoter, as described earlier for *S. cerevisiae PMR1* (11). The resulting clone, YEpPGK-KIAA0703, was unable to complement the phenotypes of a *pmr1*Δ strain and was judged to be nonfunctional. Examination of the N-terminal sequence revealed it to be similar to intronic sequences in the genome and highly hydrophobic, such that an additional membrane span would be introduced at the start of the protein, inverting the topology of the remaining membrane spans. Therefore, the N-terminal sequence of KIAA0703 was replaced with the corresponding sequence from cDNA clone DKFZp68I0955 as follows.

A 641-bp PCR product corresponding to the N terminus of cDNA clone DKFZp68I0955 from RZPD (Deutsches Ressourcenzentrum fuer Genomforschung GmbH in Berlin, Germany) was amplified using the antisense primer (GAGGTCCGTGACCTCAGTGAGTCG) and an MluI-containing sense primer (GCGCACGCGTGTCGAGGGACGaGTCTC-CGAGTTCCTGAAG; MluI site underlined; a silent mutation shown in lowercase was introduced to abolish the only internal MluI site within the hSPCA2 gene). The PCR fragment was digested with MluI and BamHI, and the resulting fragment (604 base pairs) was inserted into the same restriction sites to correct the N-terminal sequence in plasmid YEpPGK-KIAA0703 described above. It is worth noting that clone DKFZp68I0955 also carries an apparent cloning artifact in the form of an in-frame insert of 29 amino acids within the highly conserved transmembrane domain M6, not represented in the human genome sequence, and is therefore also likely to be nonfunctional. The open reading frame we have constructed from these two incorrect clones is identical to that of the recently deposited RZPD cDNA, DKFZp686H22230, except for a polymorphism at amino acid position 466 (Leu replaces Met).

Yeast strain K616 (*pmr1*Δ*pmc1*Δ*cnb1*Δ; referred as *pmr1* in the figures) has been shown to be devoid of endogenous $Ca^{2+}$-ATPase activity (6) and was used as host for heterologous expression of hSPCA1 and hSPCA2. Yeast cultures were grown in SC medium with supplements as appropriate. Where indicated, BAPTA (10 mM stock in MES, pH 6.0), $MnCl_2$ (0.5 M stock in $H_2O$), tunicamycin (20 mg/ml stock in 5 μM NaOH), and amiodarone-HCl (5 mM in dimethyl sulfoxide) were added to the cultures. Cultures were incubated at 30 °C for 72 h, and cell density was measured as $A_{600}$ in a FLUOStar Optima plate reader (BMG Labtechnologies).

*Antibody Generation and Purification*—Polyclonal antibodies were raised in rabbits against a 14-amino acid peptide of hSPCA2 ($^{30}$EEALIDEQSELKAI$^{43}$C). hSPCA2 peptide (1 mg/ml) was immobilized on SulfoLink Coupling Gel (Pierce) through the C-terminal cysteine according to the manufacturer's instructions. Peptide-specific antibodies were purified from antiserum as described (20), concentrated by Centricon filtration (YM30; Millipore Corp.), and stored in phosphate-buffered saline supplemented with 0.02% $NaN_3$ at 4 °C.

*Immunofluorescence*—Postnatal rat hippocampal neurons were a generous gift of Radhika Reddy, Richard Cho, and Paul Worley of The Johns Hopkins School of Medicine. Cultures were grown on collagen-coated glass coverslips at low densities, as described (Div 6; Ref. 21). Cells were fixed in 4% paraformaldehyde for 20 min, washed, and then permeabilized in 0.2% Triton X-100 for 10 min. Following additional washes in phosphate-buffered saline and blocking with bovine serum albumin (10% for 60 min), the coverslips were incubated with affinity-purified anti-hSPCA2 antibody (1:100 dilution), anti-TGN38 antibody (1:300; BD Transduction Laboratories), or anti-adaptin γ antibody (1:500; BD Transduction Laboratories) for 1 h. Where specified, antibody was preincubated with hSPCA2 peptide (50 μg) prior to use. Secondary antibodies used were anti-rabbit Alexa Fluor 488 (1:400; Molecular Probes) and anti-mouse Alexa Fluor 568 (1:400; Molecular Probes). Cells were imaged on a PerkinElmer UltraView spinning disk confocal microscope.

*$^{45}$Ca Transport*—ATP-dependent $^{45}$Ca transport was essentially as described (6). Concanamycin (500 nM; Sigma) and carbonylcyanide-*m*-chlorophenylhydrazone (20 μM; Sigma) were included to inhibit $H^+$/$Ca^{2+}$ exchange. $^{45}CaCl_2$ was added to 0.4 μCi/ml in transport assays of sucrose gradient fractions and to 28 μCi/ml in the pooled Golgi fraction. EGTA concentrations were varied to give free $Ca^{2+}$ concentrations that were calculated according to Wei *et al.* (11). Buffers were depleted of contaminating $Ca^{2+}$ by using Chelex-treated water. The transport assay was terminated by rapid filtration onto 0.45-μm HAWP membranes (Millipore Corp.), and radioactivity associated with vesicles was determined by scintillation counting.

*Membrane Preparation, SDS-PAGE, and Biochemical Techniques*—Yeast lysates were fractionated on 18–54% (w/w) sucrose density gradients as described (6). Protein determination by a modified Lowry assay, SDS-polyacrylamide gel electrophoresis, and Western blotting was as described (6). Anti-His antibody (1:5000; BD Biosciences) and anti-mouse IgG (1:10,000; Amersham Biosciences) were used for detection of His-tagged hSPCA2 in sucrose fractions.

## RESULTS

*Sequence Characteristics of hSPCA2*—The *ATP2C2* gene encoding hSPCA2, a second paralogue of the secretory pathway family of $Ca^{2+}$ pumps, resides on human chromosome 16. The cDNA for hSPCA2 was pieced together by replacing the incorrect N-terminal sequence from cDNA KIAA0703 with amino acid residues 1–70 from the RZPD clone DKFZp68I0955 to generate a 946-residue polypeptide with 64% sequence identity with hSPCA1 (Fig. 1). Sequences corresponding to the 10 predicted transmembrane domains and cytosolic phosphorylation and ATPase domains are strongly conserved, with significant stretches of differences residing mainly at the N and C termini. Of note, acidic residues identified as ion binding ligands within membrane spans M4, M5, and M6 in Pmr1, as well as an invariant Gln residue in M6 that is critical for $Mn^{2+}$ selectivity, are completely conserved (9, 22). A $Ca^{2+}$-binding EF-hand-like motif characterized within the N terminus of yeast Pmr1 is recognizable by conservative replacements in hSPCA1 but is considerably divergent in hSPCA2 (Fig. 1) (11). The short C terminus of hSPCA2 has a dileucine motif that may be involved in adaptor-mediated sorting and a potential type III PDZ binding motif, PEDV, at the C terminus that may be important for localization and trafficking (23, 24).

*Tissue Distribution and Subcellular Localization of hSPCA2*—Polyclonal antibodies were raised against a unique 14-residue N-terminal sequence of hSPCA2, $^{30}$EEALIDEQSELKAI$^{43}$. Affinity-purified serum recognized a 105-kDa polypeptide corresponding to hSPCA2, expressed in yeast (Fig. 2, *A* and *B*). The absence of cross-reactivity against hSPCA1 was confirmed using membranes isolated from yeast strains overexpressing the long N terminus splice variant of *ATP2C1* (14, 19). When applied to a human tissue blot, the antibodies showed prominent staining of appropriately sized bands in the brain and testis that were absent from the peptide-blocked antibody control (Fig. 2, *C* and *D*). Longer exposure times revealed weaker bands of the same size in other tissues, notably lung, kidney, and spleen (not shown). Expression profiling of KIAA0703 by RT-PCR, reported by Ishikawa *et al.* (18), showed a similar pattern of mRNA in brain, testis, lung, kidney, pancreas, and ovary. Our observations do not preclude the existence of additional splice variants that are not detected by this N-terminal antibody. Overall, the distribution of hSPCA2 appears to be considerably more restricted than that of hSPCA1 (15).

The relatively high levels of expression in the brain prompted us to examine the subcellular localization of endogenous SPCA2 in primary neuronal cell cultures from rats. Anti-hSPCA2 antibodies are expected to cross-react with the rat orthologue, since 10 of 14 residues in the epitope are identical between the two species. Rat hippocampal neurons stained with affinity-purified antibody against the N-terminal peptide of hSPCA2 showed a highly punctate distribution throughout the cell body and dendrites (Fig. 3, *a*, *d*, and *g*). An increased density of perinuclear staining of SPCA2 suggested a close association of these vesicles with the TGN. Although there was moderate overlap with TGN38 in the perinuclear stacks of the *trans*-Golgi network, we observed extensive overlap in the vesicular structures within the cell body and dendrites (Fig. 3, *d–f*). This suggested that SPCA2 localized to vesicles derived from the TGN. Indeed, we observed better colocalization between SPCA2 and adaptin-γ, a component of the AP-1 adaptor that mediates vesicle transport from the TGN to late endosomes and secretory granules (Fig. 3, *g–i*). Thus, in addition to the more compact Golgi/TGN staining of SPCA1

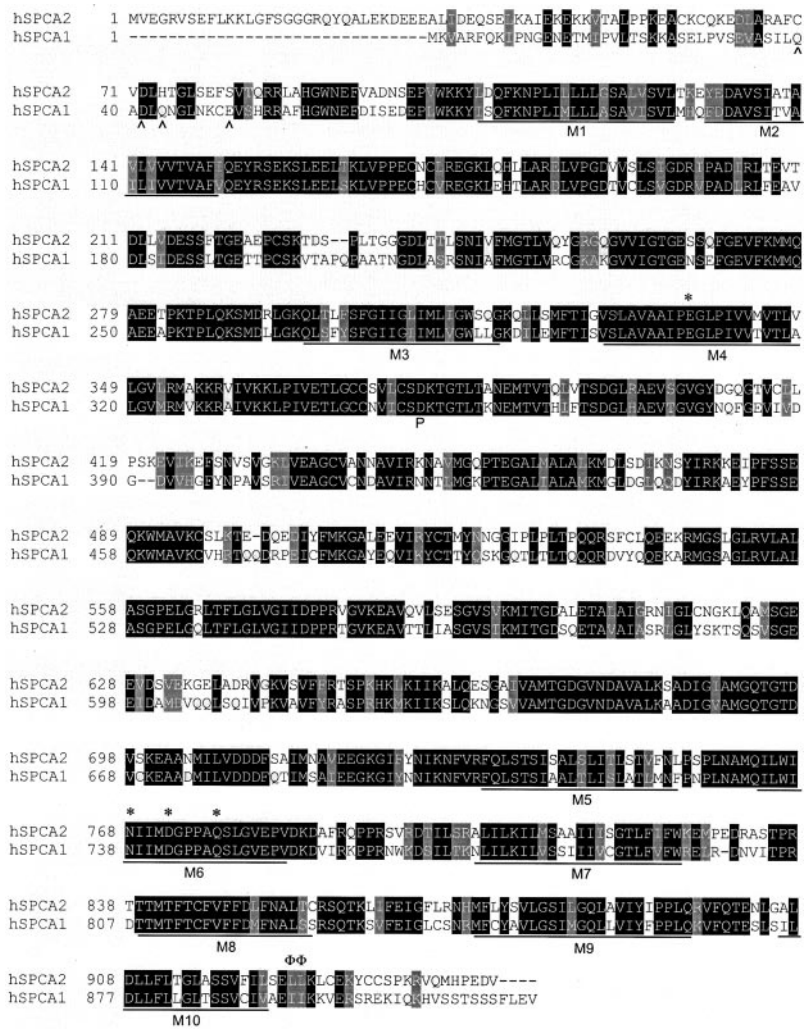


FIG. 1. **Alignment of two human SPCA isoforms.** The deduced amino acid sequence of hSPCA2 was aligned with the long isoform of hSPCA1 reported earlier (14) using ClustalW. Sequences corresponding to predicted transmembrane helices M1-M10 are *underlined*, and residues implicated in ion binding and selectivity are shown with an *asterisk*. The catalytic aspartate that is phosphorylated in P-type ATPases is indicated (*P*). The residues corresponding to an N-terminal EF-hand motif (^) and putative C-terminal retrieval motifs ($\phi\phi$) are indicated.

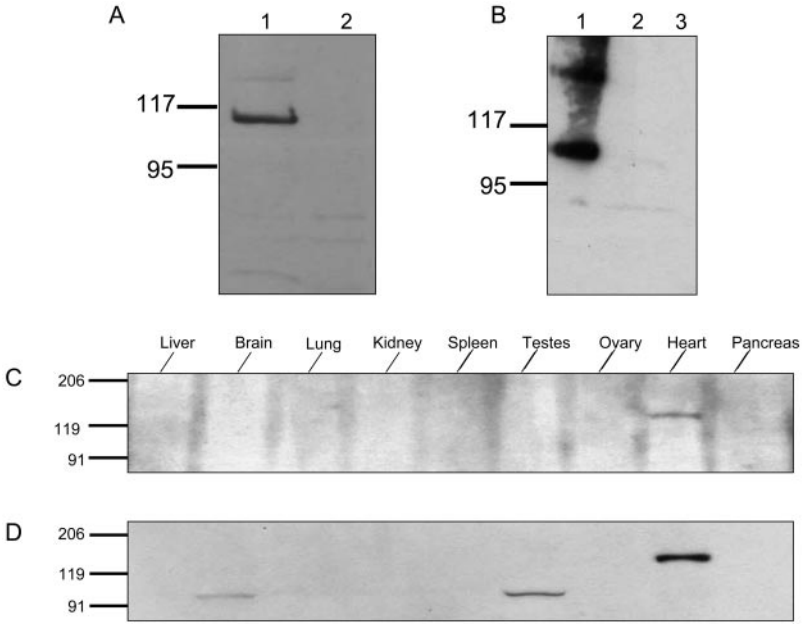


FIG. 2. **Protein expression of hSPCA2.** *A*, Western analysis of yeast membranes (50 $\mu$g) from host strain K616 (*pmr1*Δ), transformed with plasmid expressing hSPCA2, treated with affinity-purified antibody in the absence (*lane 1*) or presence of excess competing peptide (*lane 2*). *B*, Western analysis of yeast membranes (50 $\mu$g) from K616 transformed with plasmid expressing hSPCA2 (*lane 1*), hSPCA1 (*lane 2*), or neither (*lane 3*). Note the absence of cross-reactivity against hSPCA1. *C*, human multiple tissue blot (Bioworld) containing 75 $\mu$g of the tissues indicated was probed with anti-hSPCA2 antibody, preincubated with excess peptide. *D*, a separate blot as in *C*, probed with anti-hSPCA2. Longer exposures (not shown) revealed fainter bands in other tissues as described under "Results."

seen in keratinocytes and nonpolarized cells (13, 25–27), our studies reveal that SPCA pumps may localize predominantly in TGN-derived vesicles.

*Functional Complementation in Yeast*—Heterologous expression of hSPCA2 in yeast can provide valuable functional insights by complementation studies of *pmr1*Δ cellular phenotypes. The *pmr1*Δ null strain exhibits a number of growth defects deriving from the loss of high affinity $Mn^{2+}$ and $Ca^{2+}$ transport into the secretory pathway that may be complemented by expression of orthologous genes from other organ-

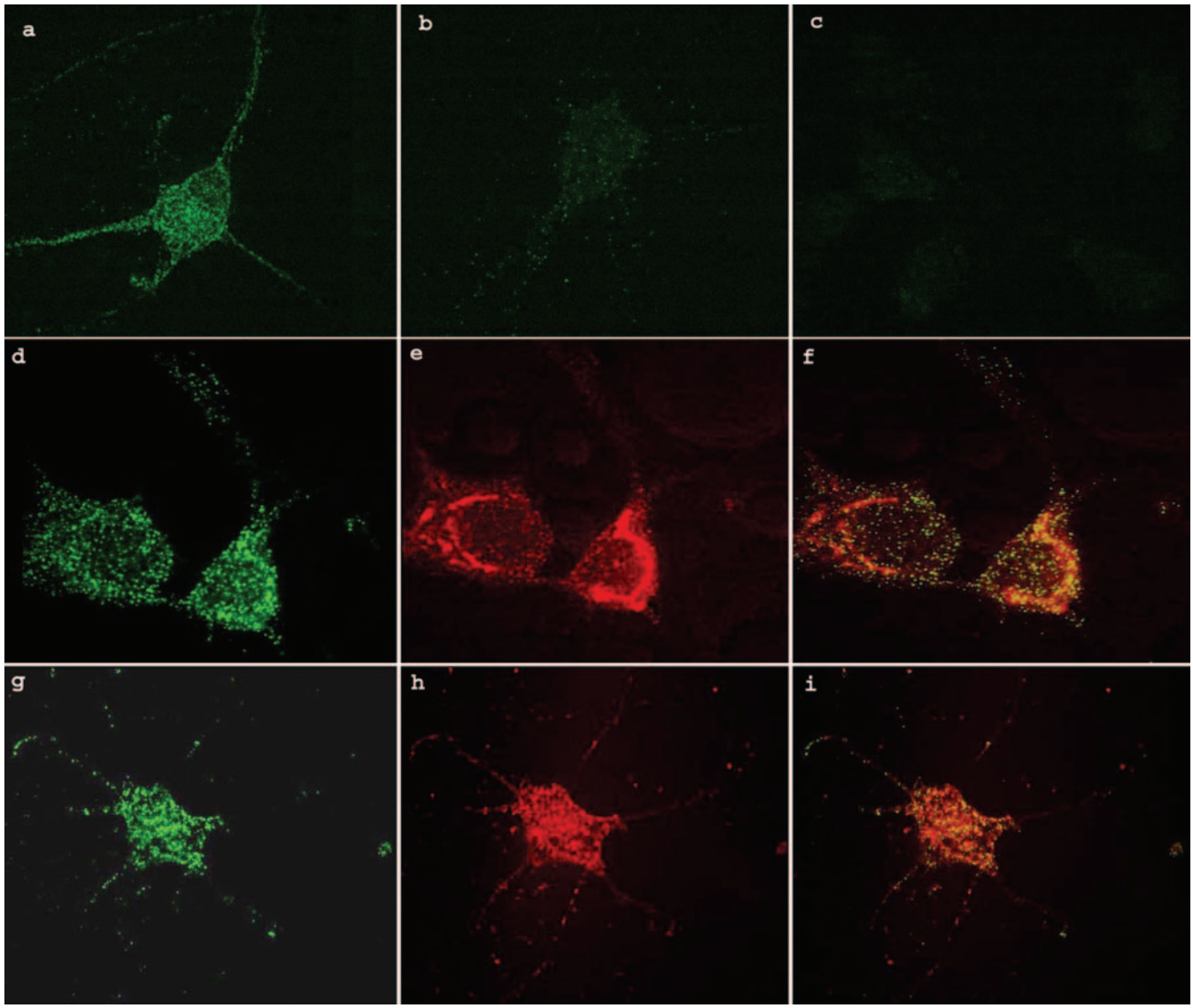


FIG. 3. **Immunofluorescence of endogenous SPCA2 in neuronal cells.** Primary cultures of mouse hippocampal neurons were treated with affinity-purified antibodies to SPCA2 (*a*, *d*, and *g*), TGN38 (*e*), and adaptin-γ (*h*) as described under "Materials and Methods." The specificity of the anti-SPCA2 antibody is demonstrated by the controls showing peptide competition (*b*) and secondary antibody alone (*c*). The highly punctate distribution of SPCA2 in the cell body and dendrites partially colocalized with TGN38 and adaptin-γ, as exemplified by the *merged images* (*f* and *i*).

isms. For example, growth sensitivity of *pmr1*Δ strains to high levels of extracellular $Mn^{2+}$ is due to cellular accumulation of $Mn^{2+}$ and can be relieved by sequestration of the toxic cation into the Golgi, from where it can exit the cell through the secretory pathway (7, 28). We had shown earlier that complementation of $Mn^{2+}$ hypersensitivity of *pmr1*Δ is a diagnostic feature of the SPCA pumps that could not be phenocopied by $Ca^{2+}$-ATPases of the SERCA or PMCA family (13). We show that hSPCA2, like hSPCA1, confers high levels of $Mn^{2+}$ tolerance to *PMR1*-deficient yeast, consistent with an ability to transport and sequester this ion (Fig. 4*A*).

In order to assess *in vivo* $Ca^{2+}$ transport activity of hSPCA2, we monitored growth sensitivity to BAPTA. Hypersensitivity of *pmr1*Δ strains to divalent cation chelators BAPTA and EGTA appears to be due to an inability to scavenge $Ca^{2+}$ ions for delivery into the endoplasmic reticulum/Golgi compartments, where they are important for protein sorting and quality control (8). Tolerance to EGTA or BAPTA can be conferred by heterologous expression of a variety of high affinity $Ca^{2+}$-transporting ATPases, including SERCA and PMCA pumps from plants, protozoans, and mammals (8, 13, 29, 30). To our surprise, hSPCA2 only weakly complemented the BAPTA-sensitive phenotype of the *pmr1*Δ strain (Fig. 4*B*), suggesting that $Ca^{2+}$ transport function was altered in some way from that of hSPCA1 and Pmr1 pumps. To corroborate this unexpected result, we also assessed tunicamycin sensitivity, which has also been shown to correlate with a depletion of calcium ions in the endoplasmic reticulum/secretory pathway (8). Yeast strains lacking Pmr1 are hypersensitive to tunicamycin due to defects in handling unfolded proteins. Again, in contrast to hSPCA1, heterologous expression of hSPCA2 only weakly complemented growth sensitivity of the host strain to tunicamycin (Fig. 4*C*), suggesting a specific deficit in calcium but not manganese sequestration. Based on these data, we reasoned that hSPCA2-transformed yeast would also be defective in cytosolic calcium homeostasis. We have recently shown that the fungicidal effect of the antiarrhythmic drug amiodarone is due to disruption of calcium homeostasis and that hypersensitivity to amiodarone in *pmr1*Δ strains correlates with loss of $Ca^{2+}$ rather than $Mn^{2+}$ transport activity (31). We show here that protection against amiodarone toxicity by hSPCA2 is significantly less than that by hSPCA1 (Fig. 4*D*), consistent with a reduced ability to clear

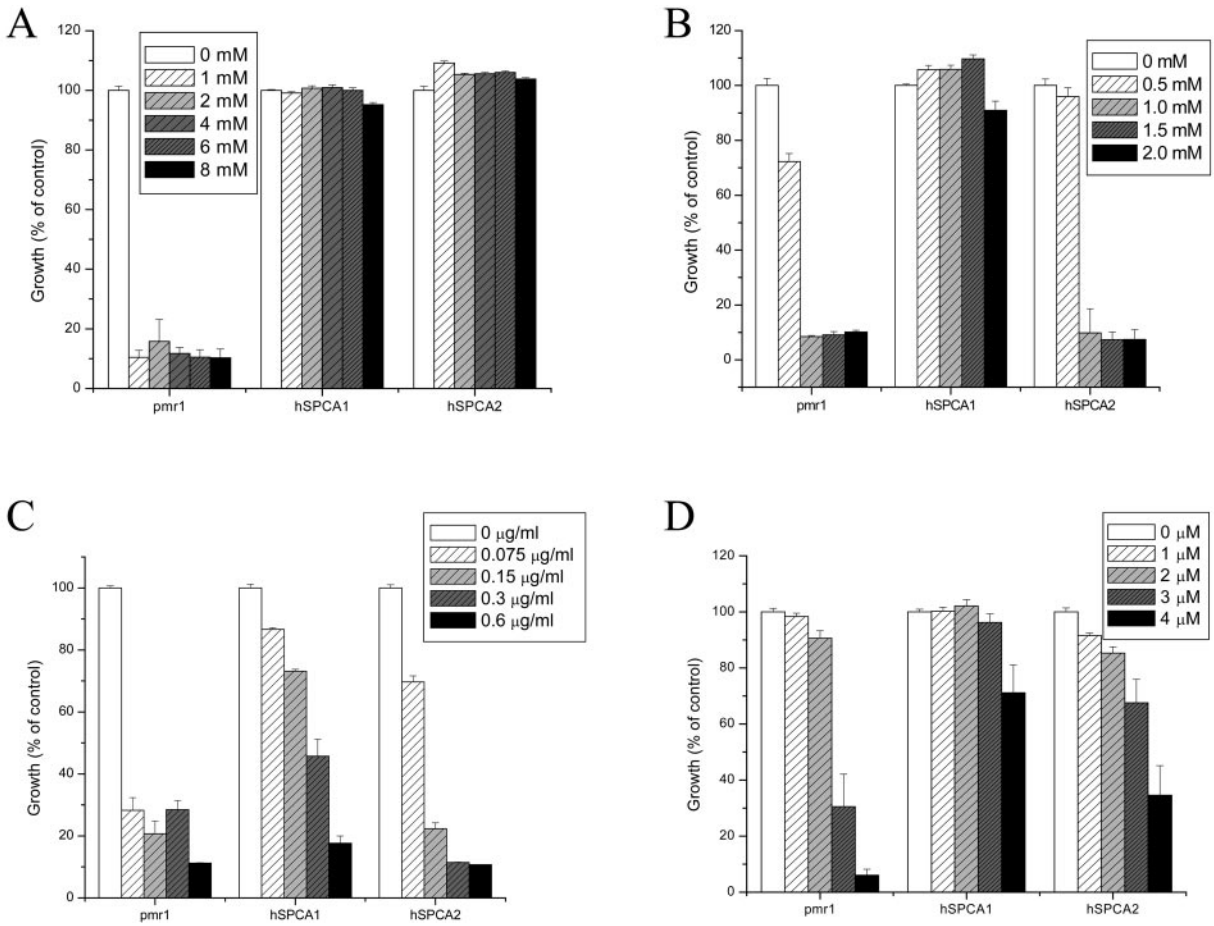


FIG. 4. **Complementation of $Ca^{2+}$ and $Mn^{2+}$ phenotypes in yeast.** Host strain K616 (*pmr1*) was transformed with plasmid expressing hSPCA1 or hSPCA2 as described under "Results." Cultures were grown in SC medium supplemented with the indicated concentrations of $MnCl_2$ (*A*), BAPTA (*B*), tunicamycin (*C*), and amiodarone-HCl (*D*). Growth ($A_{600}$) was normalized to control growth in unsupplemented medium, which was similar in all strains. Averages of triplicate measurements from a representative experiment are shown.

cytoplasmic $Ca^{2+}$. Taken together, this set of complementation studies suggest that although the $Mn^{2+}$ transport ability of hSPCA2 is similar to that of hSPCA1, $Ca^{2+}$ transport may differ.

*Golgi Localization and $^{45}Ca$ Transport*—To evaluate $Ca^{2+}$ transport activity of hSPCA2 *in vitro*, yeast lysates were separated on sucrose density gradients, and ATP-dependent $^{45}Ca$ pumping activity was determined in individual fractions. Golgi vesicles distribute in the upper third of the density gradient as seen by the peak of $^{45}Ca$ pumping activity associated with Pmr1 expression (6) (Fig. 5*A*). Introduction of hSPCA2 into the host strain lacking endogenous calcium pumps restored $Ca^{2+}$ transport activity in the Golgi-associated fractions, indicating a subcellular distribution similar to that of Pmr1 and hSPCA1 in yeast (Fig. 5*A*). Expression of hSPCA2 polypeptide was detected on Western blots of individual fractions using both anti-His and anti-hSPCA2 antibody and correlated well with $^{45}Ca$ transport activity (Fig. 5*B*). Interestingly, maximal transport activity of hSPCA2 in isolated fractions was at similar levels to hSPCA1.

Our results thus far, showing similar $Ca^{2+}$ transport activity and subcellular localization of both hSPCA1 and hSPCA2 expressed in yeast, do not explain the large disparity in $Ca^{2+}$-related growth phenotypes shown in Fig. 4, *B–D*. We therefore undertook a more detailed characterization of the ion transport activity of hSPCA2. Subcellular fractions showing peak transport activity (22–34% sucrose) were pooled and collected by centrifugation, and the calcium dependence of $^{45}Ca$ transport was determined. We show that the average $K_m$ for $Ca^{2+}$ transport by hSPCA2 is 1.35 $\mu$M, significantly different from the $K_m$ values for hSPCA1 (0.25 $\mu$M) and yeast Pmr1 (0.07 $\mu$M) measured in the same expression system (Fig. 6*A*) (11, 13). Thus, hSPCA2 appears to have poorer affinity for $Ca^{2+}$ relative to hSPCA1 and yeast Pmr1. The addition of increasing concentrations of $Mn^{2+}$ ions resulted in a corresponding decrease of hSPCA2 $Ca^{2+}$ transport activity, approaching 100% inhibition at the highest concentrations of $Mn^{2+}$ tested. Inhibition of hSPCA1 by $Mn^{2+}$ ions was very similar (13), consistent with both isoforms having similar efficacy in conferring $Mn^{2+}$ tolerance to *pmr1*Δ yeast. Although this assay does not directly measure $Mn^{2+}$ transport, prior studies have demonstrated that $Mn^{2+}$ stimulates phosphoenzyme formation and can be transported by the SPCA pumps (9, 12). Taken together, our results suggest that hSPCA2 has retained $Mn^{2+}$ pumping ability but has lost high affinity $Ca^{2+}$ transport relative to other members of the SPCA family.

## DISCUSSION

In contrast to the many decades of well documented studies that elucidate important functions of SERCA and PMCA pumps in cellular $Ca^{2+}$ homeostasis, the specific functions and *raison d'etre* of members of the SPCA class are still poorly defined. The absence of homozygous *ATP2C1* mutations in humans and the autosomal dominant mode of inheritance of Hailey Hailey disease both point to an apparent essential role for the SPCA in mammalian physiology. They may contribute to maintaining the submicromolar resting levels of cytosolic $Ca^{2+}$ prerequisite for ubiquitous signaling events, either in a

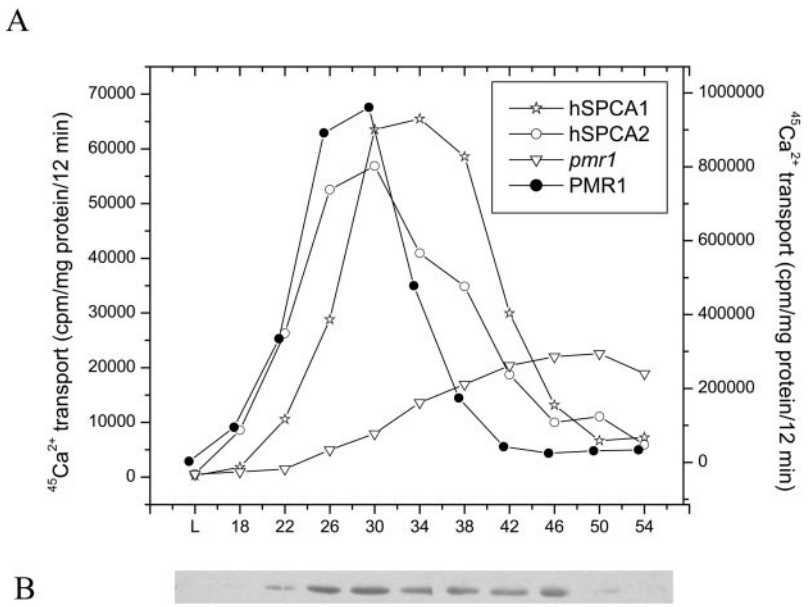


FIG. 5. **Subcellular distribution of SPCA pumps in yeast.** Yeast lysates from host strain K616 (*pmr1*), transformed with plasmid expressing hSPCA1, hSPCA2, and yeast PMR1 as indicated, were separated on sucrose density gradients (18–54% (w/w); *L* represents loading sample). *A*, ATP-dependent, carbonylcyanide-*m*-chlorophenylhydrazone-insensitive $^{45}Ca$ transport activity of fractions was measured as described (see "Materials and Methods") (6). $Ca^{2+}$ transport activity is shown on the *left axis*, *open symbols* (hSPCA1, hSPCA2, and *pmr1*) and on the *right axis*, *closed symbol* (PMR1). Peak activity of hSPCA2 coincides with PMR1 and is similar to hSPCA1. Averages of triplicate measurements from one of two independent experiments are shown; error bars are omitted for clarity. *B*, Western analysis of fractions (50 $\mu$g) from strain K616 expressing hSPCA2, probed with anti-His antibody. Note that fractions containing the highest activity (26 and 30%) in *A* also have the highest hSPCA2 expression.

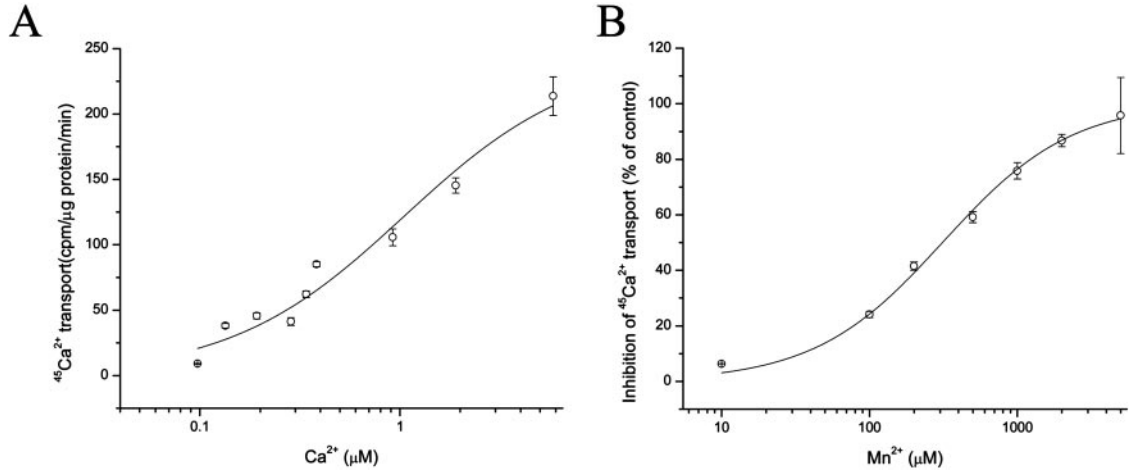


FIG. 6. **Cation dependence of $^{45}Ca$ transport activity of hSPCA2.** Golgi membranes, showing peak $^{45}Ca$ transport activity from sucrose gradients, were collected as described under "Materials and Methods," and ATP-dependent, protonophore-insensitive $^{45}Ca$ transport activity was determined. *A*, affinity for $Ca^{2+}$ was determined by varying EGTA concentrations to give the free calcium ion concentrations shown. Triplicate determinations from one of two independent preparations are shown. Data were fitted to the Michaelis-Menten equation using Origin software. Half-maximal transport activity was at 1.1 $\mu$M ($r = 0.98$). The second preparation gave a $K_m$ of 1.6 $\mu$M for $Ca^{2+}$, with a similar $r$ value. *B*, $Mn^{2+}$ inhibition of $^{45}Ca$ transport activity in pooled Golgi membranes was demonstrated by adding the indicated concentrations of $MnCl_2$ to the $^{45}Ca$ transport medium (see "Materials and Methods"). Note that the assay does not directly measure affinity for $Mn^{2+}$ but indicates the ability of $Mn^{2+}$ to effectively inhibit $^{45}Ca$ transport, similar to previous observations with hSPCA1 (13).

supporting role or more prominently in some cell types such as keratinocytes where Hailey Hailey disease is manifested (32). Luminal delivery of ions to Golgi and post-Golgi compartments for protein processing, glycosylation, and secretion is more likely to be a specific function of the SPCA, particularly in vesicles where overlap with the SERCA would be minimal.

The high $Mn^{2+}$ selectivity of the SPCA is not only unique among other classes of $Ca^{2+}$-ATPases but serves as a defining characteristic common to all members that have been investigated thus far, including the newly identified hSPCA2 isoform reported in this study. We show that like hSPCA1, hSPCA2 confers robust tolerance to $Mn^{2+}$ toxicity in yeast and is therefore a candidate for $Mn^{2+}$ uptake or detoxification in tissues in which it is expressed. The relatively high level of hSPCA2 in brain is particularly intriguing, given the observed correlations between manganese neurotoxicity and Parkinson's disease (33). Manganese is an abundant element that is widely used in industrial applications, including the manufacture of steel and batteries and as an anti-knock additive of gasoline. There is considerable evidence that excessive exposure to $Mn^{2+}$, particularly when inhaled or in patients with liver disease, causes neuronal loss and gliosis that is most prominent in the globus pallidus and substantia nigra (33–35). Our studies showing SPCA2 expression in neuronal cells are consistent with a role in $Mn^{2+}$ sequestration and detoxification, similar to that in yeast. In support of this function, a recent study documenting protein expression changes in rat brains following manganese exposure showed a prominent up-regulation of an SPCA member (36).

Given the ubiquitous occurrence of hSPCA1, the more limited distribution of hSPCA2 would suggest a specialized role. Indeed, the relatively poor affinity for $Ca^{2+}$ indicates that this isoform may participate primarily in $Mn^{2+}$ transport in a cellular context, although we cannot rule out factors such as accessory proteins, phosphorylation, or other forms of regulation that may be absent in a heterologous system but serve to modulate ion affinity. The difference in $Ca^{2+}$ transport affinity

between hSPCA2 and other members of the SPCA family is surprising, given the high level of sequence identity in membrane-spanning regions that are known to bind and transport ions. Sequences corresponding to M4, M5, and M6 in both human isoforms are virtually identical, with few conservative replacements, and all critical residues identified in yeast mutagenesis screens or in Hailey Hailey disease are conserved (*2*). Therefore, it would appear that regions outside these core membrane helices modulate ion binding and transport.

It is possible that the divergent N-terminal sequences of the SPCA pumps serve to modulate ion affinity. An EF-hand motif located within the N-terminal sequence of yeast Pmr1 has been shown to bind $Ca^{2+}$, and mutations that abolish $Ca^{2+}$ binding to a fusion of the N terminus with glutathione *S*-transferase also reduced affinity for $Ca^{2+}$ transport in the full-length pump (11). We note a correlation between the degree of conservation of the EF-hand motif and the apparent affinity for $Ca^{2+}$ transport. Thus, the sequence D*X*D*X*N*X*G*X*$_5$E in Pmr1 resembles canonical EF hands better than that of hSPCA1, Q*X*D*X*Q*X*G*X*$_4$E, whereas the equivalent sequence in hSPCA2 has several nonconservative replacements lacking $Ca^{2+}$-binding carbonyl groups (underlined), C*X*D*X*H*X*G*X*$_4$S. There is precedence for N-terminal sequences modulating ion transport in the related $P_1$ subtype of P type ion pumps, which include the copper-ATPases defective in Menkes and Wilson disease. In these pumps, 1–6 discrete metal binding motifs within the long N terminus are thought to regulate ion transport (37). Although similar modulation by N-terminal sequences has not been reported for pumps of the $P_2$ subtype, which include $Ca^{2+}$-ATPases, it remains an intriguing possibility.

We demonstrate, for the first time, a predominantly vesicular distribution for a member of the SPCA subgroup, distinct from the compact perinuclear Golgi/TGN stacks observed for SPCA1 in keratinocytes and nonpolarized cultured cells. It is likely that the distribution of the SPCA between TGN stacks and TGN-derived vesicles is cell type-dependent and may reflect the balance between export and retrieval of the pumps. It will be of particular interest to determine whether this distribution is $Ca^{2+}$- or $Mn^{2+}$-dependent and whether C-terminal motifs associated with PDZ domain binding (PEDV) and retrieval from the plasma membrane (LL) contribute to trafficking. Again, there is precedence for ion-dependent Golgi to vesicular trafficking in the Menkes and Wilson copper ATPases, where similar motifs have been identified (38).

In summary, we identify a distinct mammalian member of the family of secretory pathway pumps with novel properties that include a more limited tissue distribution, localization to TGN-derived vesicles in neuronal cells, a poorer affinity for calcium ions, and distinct phenotypic effects in yeast. Taken together, these findings indicate that hSPCA2 may have a more specialized cellular role, possibly including delivery and detoxification of $Mn^{2+}$ in the TGN and endosomal compartments.

*Acknowledgments*—We thank Radhika Reddy and Richard Cho (The Johns Hopkins University) for generous gifts of neuronal cells and valuable advice.

REFERENCES

1. Wuytack, F., Raeymaekers, L., and Missiaen, L. (2003) *Pflugers Arch. Eur. J. Physiol.* **446,** 148–153
2. Ton, V. K., and Rao, R. (2004) *Am. J. Physiol. Cell Physiol.* **287,** C580-C589
3. Rudolph, H. K., Antebi, A., Fink, G. R., Buckley, C. M., Dorman, T. E., LeVitre, J., Davidow, L. S., Mao, J. I., and Moir, D. T. (1989) *Cell* **58,** 133–145
4. Antebi, A., and Fink, G. R. (1992) *Mol. Biol. Cell.* **3,** 633–654
5. Gunteski-Hamblin, A. M., Clarke, D. M., and Shull, G. E. (1992) *Biochemistry* **31,** 7600–7608
6. Sorin, A., Rosas, G., and Rao, R. (1997) *J. Biol. Chem.* **272,** 9895–9901
7. Lapinskas, P. J., Cunningham, K. W., Liu, X., Fink, G. R., and Culotta, V. (1995) *Mol. Cell. Biol.* **15,** 1382–1388
8. Dürr, G., Strayle, J., Plemper, R., Elbs, S., Klee, S. K., Catty, P., Wolf, D. H., and Rudolph, H. K. (1998) *Mol. Biol. Cell* **9,** 1149–1162
9. Mandal, D., Woolf, T., and Rao, R. (2000) *J. Biol. Cell* **273,** 23933–23938
10. Bolton, E. C., Mildvan, A. S., and Boeke, J. D. (2002) *Mol Cell.* **9,** 879–889
11. Wei, Y., Marchi, V., Wang, R., and Rao, R. (1999) *Biochemistry* **38,** 14534–14541
12. Van Baelen, K., Vanoevelen, J., Missiaen, L., Raeymaekers, L., and Wuytack, F. (2001) *J. Biol. Chem.* **276,** 10683–10691
13. Ton, V. K., Mandal, D., Vahadji, C., and Rao, R. (2002) *J. Biol. Chem.* **277,** 6422–6427
14. Fairclough, R. J., Dode, L., Vanoevelen, J., Andersen, J. P., Missiaen, L., Raeymaekers, L., Wuytack, F., and Hovnanian, A. (2003) *J. Biol. Chem.* **278,** 24721–24730
15. Hu, Z., Bonifas, J. M., Beech, J., Bench, G., Shigihara, T., Ogawa, H., Ikeda, S., Mauro, T., and Epstein, E. H., Jr. (2000) *Nat. Genet.* **24,** 61–65
16. Sudbrak, R., Brown, J., Dobson-Stone, C., Carter, S., Ramser, J., White, J., Healy, E., Dissanayake, M., Larregue, M., Perrussel, M., Lehrach, H., Munro, C. S., Strachan, T., Burge, S., Hovnanian, A., and Monaco, A. P. (2000) *Hum. Mol. Genet.* **9,** 1131–1140
17. Reinhardt, T. A., Filoteo, A. G., Penniston, J. T., and Horst, R. L. (2000) *Am. J. Physiol. Cell Physiol.* **279,** C1595–C1602
18. Ishikawa, K., Nagase, T., Suyama, M., Miyajima, N., Tanaka, A., Kotani, H., Nomura, N., and Ohara, O. (1998) *DNA Res.* **5,** 169–176
19. Ton, V. K., and Rao, R. (2004) *J. Investig. Dermatol.* **23,** 1192–1194
20. Dumont, R. A., Lins, U., Filoteo, A. G., Penniston, J. T., Kachar, B., and Gillespie, P. G. (2001) *J. Neurosci.* **21,** 5066–5078
21. Liao, D., Zhang, X., O'Brien, R., Ehlers, M. D., Huganir, R. L. (1999) *Nat. Neurosci.* **2,** 37–43
22. Wei, Y., Chen, J., Rosas, G., Tompkins, D. A., Holt, P. A., Rao, R. (2000) *J. Biol. Chem.* **275,** 23927–23932
23. Heilker, R., Manning-Krieg, U., Zuber, J. F., and Spiess, M. (1996) *EMBO J.* **15,** 2893–2899
24. Wang, P., Wang, X., and Pei, D. (2004) *J. Biol. Chem.* **279,** 20461–20470
25. Missiaen, L., Vanoevelen, J., Van Acker, K., Raeymaekers, L., Parys, J. B., Callewaert, G., Wuytack, F., and De Smedt, H. (2002) *Biochem. Biophys. Res. Commun.* **294,** 249–253
26. Behne, M. J., Tu, C. L., Aronchik, I., Epstein, E., Bench, G., Bikle, D. D., Pozzan, T., and Mauro, T. M. (2003) *J. Invest. Dermatol.* **121,** 688–694
27. Van Baelen, K., Vanoevelen, J., Callewaert, G., Parys, J. B., De Smedt, H., Raeymaekers, L., Rizzuto, R., Missiaen, L., and Wuytack, F. (2003) *Biochem. Biophys. Res. Commun.* **306,** 430–436
28. Mandal, D., Rulli, S. J., and Rao, R. (2003) *J. Biol. Chem.* **278,** 35292–35298
29. Liang, F., and Sze, H. (1998) *Plant Physiol.* **118,** 817–825
30. Talla, E., de Mendonca, R. L., Degand, I., Goffeau, A., and Ghislain, M. (1998) *J. Biol. Chem.* **273,** 27831–27840
31. Gupta, S. S., Ton, V. K., Beaudry, V., Rulli, S., Cunningham, K., and Rao, R. (2003) *J. Biol. Chem.* **278,** 28831–28839
32. Callewaert, G., Parys, J. B., De Smedt, H., Raeymaekers, L., Wuytack, F., Vanoevelen, J., Van Baelen, K., Simoni, A., Rizzuto, R., and Missiaen, L. (2003) *Cell Calcium* **34,** 157–162
33. Olanow, C. W. (2004) *Ann. N. Y. Acad. Sci.* **1012,** 209–223
34. Pal, P. K., Samii, A., and Calne, D. B. (1999) *Neurotoxicology* **20,** 227–238
35. Burkhard, P. R., Delavelle, J., Du Pasquier, R., and Spahr, L. (2003) *Arch. Neurol.* **60,** 521–528
36. Zhang, S., Fu, J., Zhou, Z. (2005) *Toxicol. Appl. Pharmacol.* **202,** 13–17
37. Huster, D., and Lutsenko, S. (2003) *J. Biol. Chem.* **278,** 32212–32218
38. Greenough, M., Pase, L., Voskoboinik, I., Petris, M. J., O'Brien, A. W., and Camakaris, J. (2004) *Am. J. Physiol.* **287,** C1463–C1471